Sensors and Actuators A 211 (2014) 19–26

Contents lists available at ScienceDirect

Sensors and Actuators A: Physical

journal homepage: www.elsevier.com/locate/sna

Acoustic mixer using low frequency vibration for biological and chemical applications

Faten Kardous[a,b,*], Réda Yahiaoui[c], Boujemâa Aoubiza[d], Jean-François Manceau[c]

[a] Nanotechnology Group, INSAT, Bp 676, Centre Urbain Nord, 1080 Charguia Cedex, Tunisia
[b] Nanomedicine Lab, Imagery and Therapeutics, Université de Franche-Comté Besançon, France
[c] Institut FEMTO-ST, Université de Franche-Comté, CNRS, ENSMM, UTBM, F-25044 Besançon, France
[d] Laboratoire de Mathématiques Université de Franche-Comté, CNRS, Besançon, France

ARTICLE INFO

Article history:
Received 20 September 2013
Received in revised form 26 February 2014
Accepted 1 March 2014
Available online 12 March 2014

Keywords:
Microdroplet mixing
Acoustic mixing
Thermal acoustic effect

ABSTRACT

Liquid mixing at micro-scale is considered a challenge which is even tougher to overcome in the case of discrete microfluidic. Many researchers have developed strategies and tried to be pioneer in mixing solutions for lab on chip. In this paper, we present a parallel microdroplet mixer based on acoustic field generation using a low frequency vibration (up to few hundreds of kilohertz). This device can be used for lab on chip applications, since the liquid characteristics are not disturbed by the plugged energy and involve relatively simple microfabrication techniques. We designed, fabricated, evaluated, presented experiments showing the microdroplet active mixing, and investigated the thermal effect of the created acoustic energy.

1. Introduction

Liquid mixing is usually achieved in continuous flows via liquid injection in the same micro-channel [1]. Nevertheless, at micro- and nano-scale, liquid mixing is a difficult challenge. In fact, in these cases Reynolds number R_e is doubly reduced by characteristic length and speed decrease:

$$R_e = \frac{\rho_0 \cdot \nu \cdot L}{\mu} \quad (1)$$

where ρ_0 is density, ν is liquid speed, L is characteristic length and μ is liquid viscosity. ρ_0 and μ are supposed to be independent from scale changing.

The low noted Reynolds number reflects an absence of turbulence in the channel, thus a low mixing efficiency. To overcome this difficulty, researchers added an additional energy source to introduce an active mixing by creating flow instabilities.

For example, in order to decrease mixing time and improve the continuous-flow mixture homogeneity, they developed ultrasonic mixers using stationary wave patterns or Surface Acoustic Waves (SAW) [2–5]. They equally used other energies with the same aim such as pressure field [6,7], electric field [8,9], or magnetic field variation [10]. However, continuous flow systems are limited in term of maximum number of micro-channels which are realizable despite the significant progress in micro-fabrication technologies. This limitation is pricey in biological and chemical domains, since the number of simultaneously treatable samples is low. To exploit a larger number of samples, they proposed an alternative approach to continuous microfluidic systems by manipulating discrete droplets.

To create flow instabilities in droplet, many techniques can be used like the methodology for introducing thorough chaotic mixing in microdroplets by moving it along a two-dimensional path, which are presented by some studies [11].

Paik et al. developed an electrowetting-based linear-array droplet mixer. In this device, the droplets act as virtual mixing chambers, and mixing occurs by transporting the droplet across an electrode array thanks to an electrostatic field [12].

Droplet mixing was equally performed using electrically tunable superhydrophobic nanostructured surfaces. By applying electrical voltage and current, droplets can be reversibly switched from a wetting to a non-wetting state, which induces fluid motion within the droplet [13].

A different approach can be the use of Magneto Hydrodynamic (MHD) principle. In fact, a MHD driven microfluidic system was developed to transport and mix two or more microdroplets [14].

We can also imagine introducing superparamagnetic microparticles inside the droplet so they can be afar controlled by an

* Corresponding author at: Nanotechnology Group, INSAT, Bp 676, Centre Urbain Nord, 1080 Charguia Cedex, Tunisia. Tel.: +216 55280785.
E-mail addresses: faten1_kardous@yahoo.com, fk.professionnel@gmail.com (F. Kardous).

http://dx.doi.org/10.1016/j.sna.2014.03.003
0924-4247/

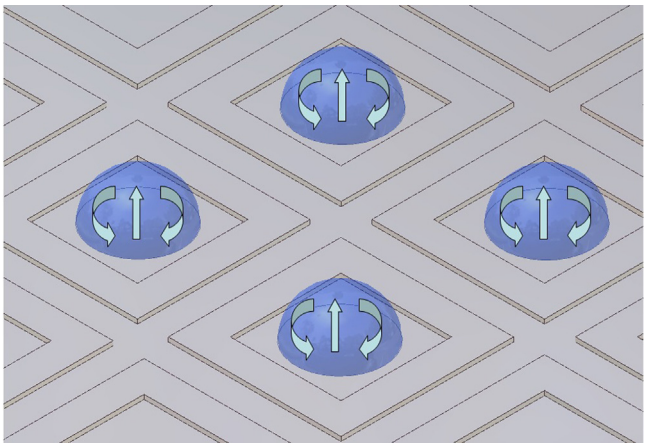

Fig. 1. Schema of hydrodynamic flow induced acoustically into many microdroplets simultaneously.

external magnetic energy. Particle movement induces a flow into the drop and as a result gets it mixed [15].

Acoustic fields can also be used for that function; several examples have been presented using, for the most part, high frequency vibrations generated by SAW devices [16].

In this paper, we propose a parallel microdroplet acoustic mixer using low frequency vibration (up to hundreds kilohertz). The device creates an active mixing in up to 25 microdroplets simultaneously. Those samples are deposited directly on the mixer vibrating surface which we designed to avoid contamination. Since the acoustic energy induces a thermal effect in liquid, we investigate this phenomenon. The designed acoustic mixer has proven its efficiency in the biological domain on Antibodies' immobilization and Antigenic reaction [17,18].

2. Design and fabrication of the acoustic mixer

2.1. Acoustic mixer working principle

Thanks to a piezoelectric ceramic, our low frequency acoustic mixer consists essentially of a thin vibrating membrane on which microdroplets are deposited. When this latter is excited at a resonance frequency, a radiation pressure is generated in each microdroplet, making hydrodynamic flow and thus mixing as shown in Fig. 1. Eventual particles introduced in a microdroplet, for example biologic entities, will follow flow lines from the drop center to the surface. Particle velocity increases with the excitation voltage for a given vibration frequency. This strategy is very interesting since the liquid characteristics are not disturbed which is an important asset for chemical and biological applications. The present acoustic mixer is designed to induce internal flows simultaneously in a matrix of microdroplets as presented in Fig. 1.

2.2. Acoustic mixer design

Our acoustic mixer results from the assembly of a silicon structure and a bulk piezoelectric ceramic. Because we intended to experiment our mixer in biological domain, the silicon structure (Fig. 2) has to be adapted to the characterization apparatus Biacore 2000 and to its corresponding SPR biochip. As a result, the mixer active surface is delimited to the Biacore sensing area. It follows a 12 mm × 12 mm active surface (membrane in Fig. 2). The vibrating membrane is centered in a much rigid substrate permitting to localize energy only in the interesting zone.

Subsequently, as microdroplets have to be easily positioned as a 5 × 5 matrix on the transducer active area, we first had to mark

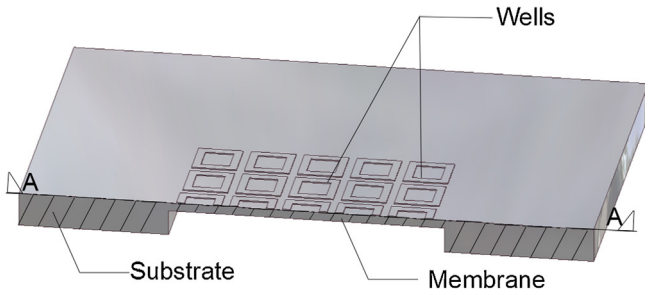

Fig. 2. Description of the silicon structure of the acoustic transducer – Cut along A–A.

the desired positions and to prevent eventual contamination due to the acoustic plugged energy. In fact, in the biological domain, discrete microfluidic is generally used to manipulate different samples (provided from different biologic solutions) which mean that any contact between microdroplets is considered as contamination. In our case, when high acoustic field intensity is applied, unwanted sample displacement and merging can thus appear. The contamination risk is particularly important since the distance between samples is small. So, to avoid contamination and provide position marks, the acoustic transducer surface was structured: 25 wells were etched in order to delimit and separate microdroplets (Fig. 2). The well dimensions are determined by the volume (600 nL) and the maximum number of microdroplets (25 microdroplets). Each well is square shaped with an inner dimension of 1.15 mm, and an outer dimension of 1.95 mm. The choice of square shaped wells results from our desire to adopt KOH etching microfabrication technique in order to ensure the simplest fabrication process. Well height is determined to be sufficient to spatially isolate drops and low enough to conserve low frequency vibration. ANSYS Multiphysics simulations of the entire structure permitted to choose 50 μm well heights. The active surface is excited by a massive piezoelectric ceramic as shown in Fig. 3.

2.3. Acoustic transducer micro-fabrication

The silicon structure was made using microfabrication techniques. First, a 100 μm-thick membrane is obtained by etching, in aqueous KOH, 500 μm-thick highly resistive silicon wafer. A second etching creates wells and incidentally makes the membrane thinner (membrane final thickness 50 μm). A 12 mm × 12 mm × 50 μm square membrane surrounded by a 25 mm × 30 mm × 450 μm rectangular substrates is achieved. To make interconnections with the piezoceramic easier, contact electrodes are incorporated to the vibrating membrane frame. For that purpose, deoxidation followed by oxidation is the key step to ensure insulation between electrodes on the transducer back side and biocompatibility on the top side. The electrode insulation is particularly better as the wafer is highly

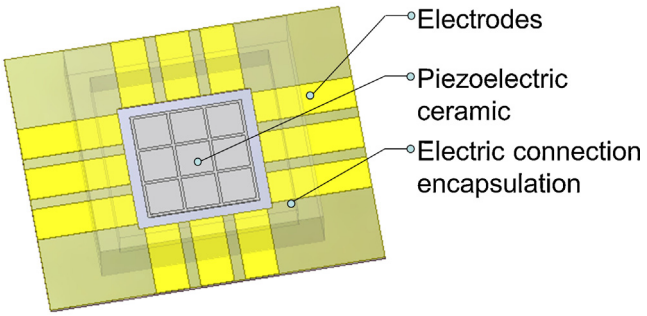

Fig. 3. Description of the acoustic transducer – bottom side.

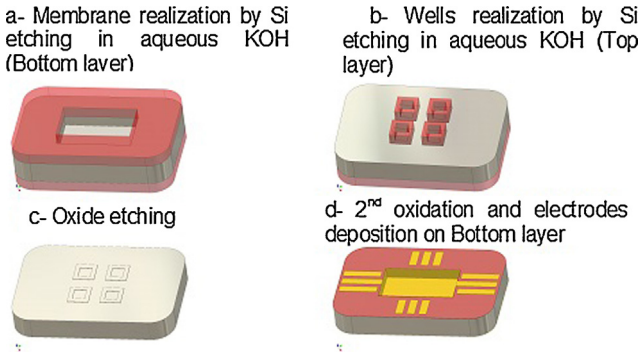

Fig. 4. Key steps of the mixer flow chart.

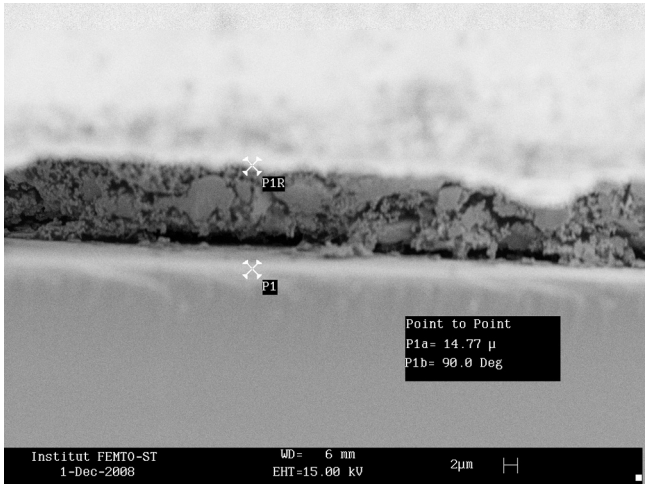

Fig. 5. The obtained thin epoxy conducting resin gluing the piezoceramic to the silicon structure (14 μm thick layer); characterization by SEM 440 Leica.

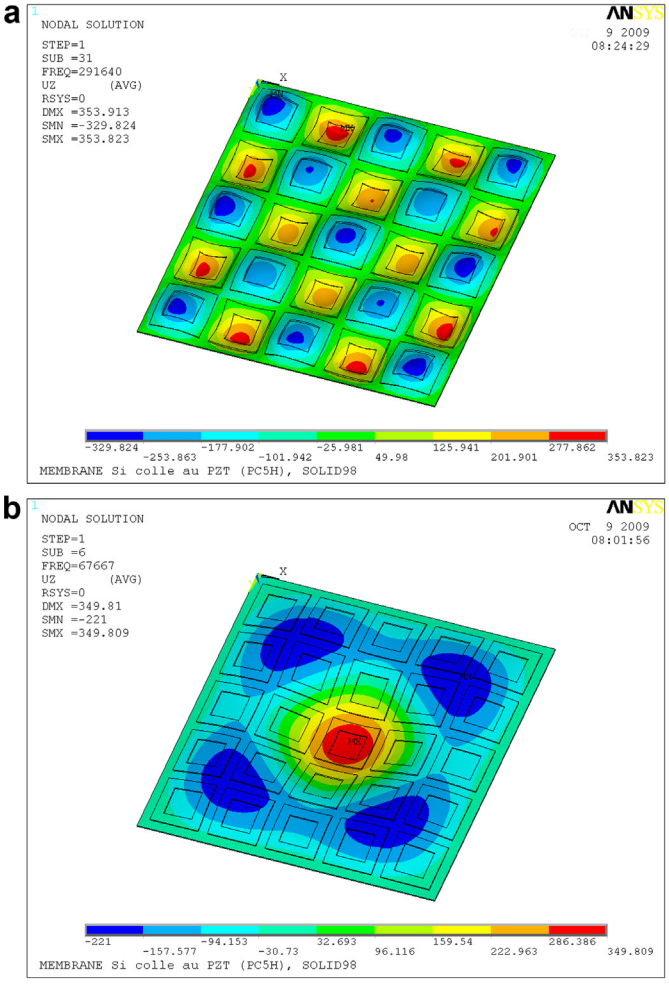

Fig. 7. ANSYS FEM modeling of the membrane (considering wells and the glued piezoceramic) a – (5, 5) mode at 291.64 kHz and b – (1, 3) + (3, 1) mode at 67.667 kHz.

resistive. A sputtered 0.5 μm thick gold layer is then structured by wet etching in order to obtain contact electrodes. Fig. 4 presents the main process steps.

Afterwards, a massive 10 mm × 10 mm × 127 μm piezoelectric ceramic (PSI-5A4E) is centered and glued to the membrane bottom side using EPOTEK E205 conductive epoxy heated at 80 °C. The obtained epoxy film joining PZT ceramic to the silicon structure is about 14 μm-thick as shown in Fig. 5, image acquired by Scanning Electron Microscope (SEM 440 Leica, 6 nm resolution at 30 KeV). The obtained assembly is then mounted on a printed circuit board. Electrical connections are performed using the ball bonding technique. The obtained low frequency vibration mixer is given by Fig. 6.

3. Experimentation

3.1. Structure vibration mode characterization

A vibration mode is determined by a pair of integers (m, n) corresponding to anti-node number, respectively, along the 'x' and 'y' directions. Fig. 7a presents the (5, 5) structure vibration mode simulated using ANSYS Multiphysics. This mode is particularly interesting when manipulating 25 samples (i.e. all wells are occupied) because it concentrates vibration on each well. This mode is expected at about 292 kHz. When only 5 samples are needed to be mixed, we chose to excite the transducer with a combination of modes (1, 3) and (3, 1). In fact, when few samples are used, lower

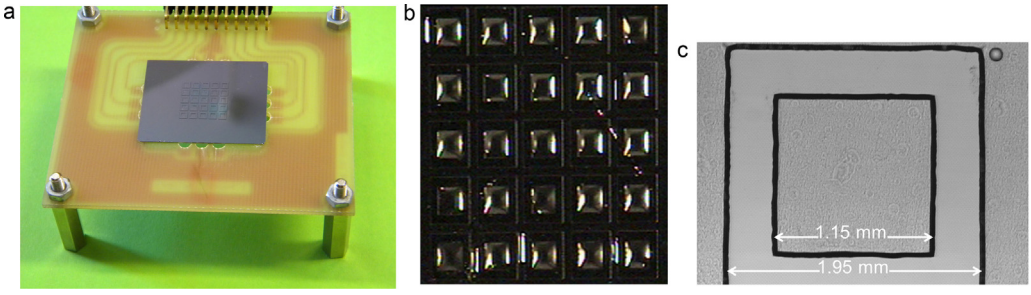

Fig. 6. Acoustic transducer for microdroplets mixing; (a) mixer photography; (b) 5 × 5 droplets spotted in the well matrix; (c) zoom on a well.

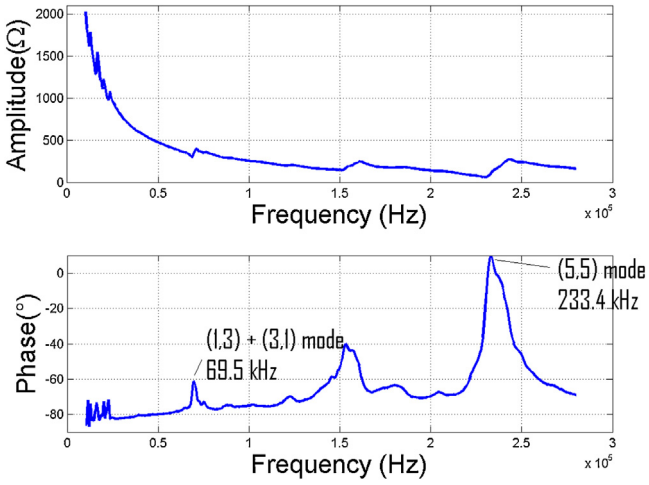

Fig. 8. Phase characteristic of the acoustic mixer: degenerated (1, 3)+(3, 1) mode noted at 69.5 kHz and (5, 5) vibration mode at 233.4 kHz.

frequency modes are preferred because they require less excitation energy. In this case, samples are deposited in wells (2, 2), (2, 4), (3, 3), (4, 2), (4, 4). Simulation reported in Fig. 7b predicts a vibration frequency of about 68 kHz for this particular vibrating mode.

The mixer is characterized with an impedance analyser (Agilent 4395A) in order to find out the vibration mode frequencies experimentally. Phase characteristic (Fig. 8) shows the presence of some modes in the interesting interval. BMI optical interferometer scanning permits simulation confirmation. Indeed, the (5, 5) mode appears at 233 kHz and the 5th degenerated mode at 69.5 kHz (Fig. 9). Deviation between simulations and measurements is probably due to some fabrication defects, but principally to the non-consideration of the glue layer in the ANSYS model.

3.2. Acoustic mixer efficiency

3.2.1. Validation of acoustic mixing

To evaluate mixing efficiency of the acoustic mixer, we have tested the device on a couple of reagents whose viscosities are very different (water and 40% glycerol in water). Actually, viscosity dramatically slows molecular diffusion which makes mixing a very slow and difficult operation espacially in microfluidic condition. To make a visual contrast between reagents and rhodamine,

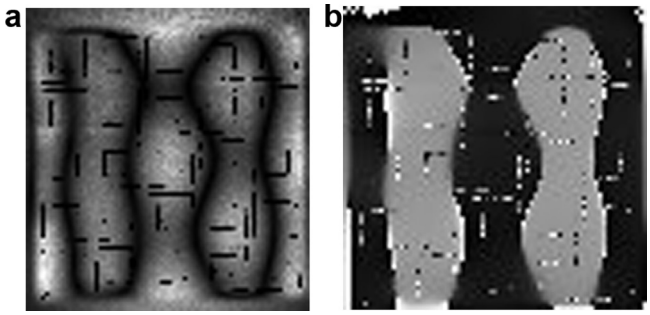

Fig. 9. Experimental vibration observed by BMI optical probe; (1, 3)+(3, 1) degenerated mode at 69.5 kHz: (a) amplitude, (b) phase.

a colorimetric probe is used. This molecule was exclusively used here to allow mixing visualization and such effect is expected for bio-macromolecules mixing in droplets.

Thereafter, rhodamine homogenization is highly concentrated in glycerol sample. Two reagents 'A' (water droplet containing rhodamine probe) and 'B' (40%, v/v glycerol concentation in water) are deposited inside the central well of the mixer vibrating membrane. Fig. 10 presents the achieved mixing sequence. In passive mode ($t < 0$), high viscosity of reagent 'B' blocked the mixing process with reagent 'A' as expected. In fact, no spontaneous mix was noted when the acoustic mixer was not excited during the first 47 s following its depositions, while this immiscibility was overcome using acoustic field. When acoustic energy was plugged into the liquid, drastic acceleration of the mixing phenomenon was observed. In less than 60 s, most of the volume has been significantly homogenized and a rhodamine uniform repartition was observed in few minutes.

To investigate particle behavior in microdroplet under acoustic mixing, 5–15 nm particles are integrated into the liquid (20% glycerol concentration in water). Then, this latter is agitated with a vortex machine before pipetting sample to avoid particle agglomeration. Afterwards, a new 400 nL microdroplet is pipetted and placed in the central well in each new characterization under specific excitation parameters.

To zoom on the drop and register particle movement, a microscope mounted CCD camera is used. Obtained videos are then digitized at 25 frames per second. Corresponding to the particles final position frame is then compared to a reference frame, corresponding to the initial steady state. Later, particle displacements

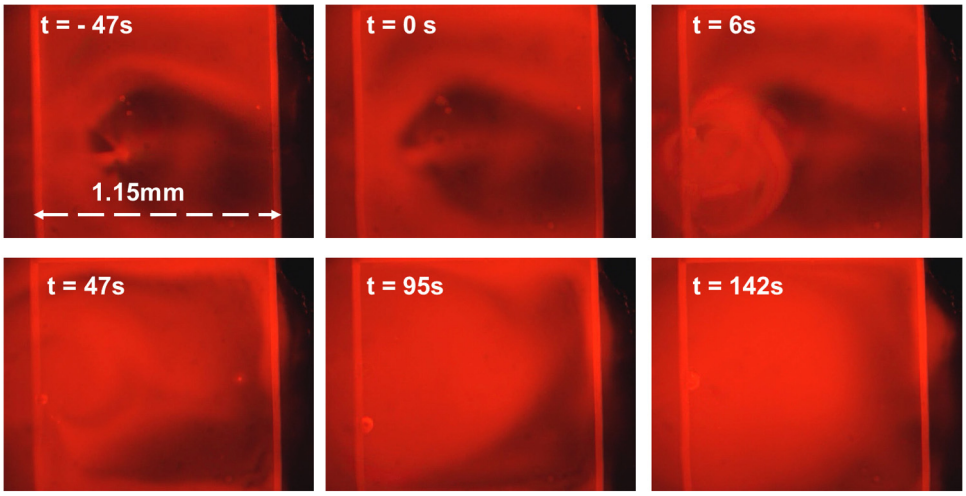

Fig. 10. Recording of acoustic mixing of A and B reagents: $t < 0$ without acoustic excitation, $t > 0$ with acoustic excitation. Reagent A: water droplet containing rhodamine probe, Reagent B: 40% glycerol concentration in water.

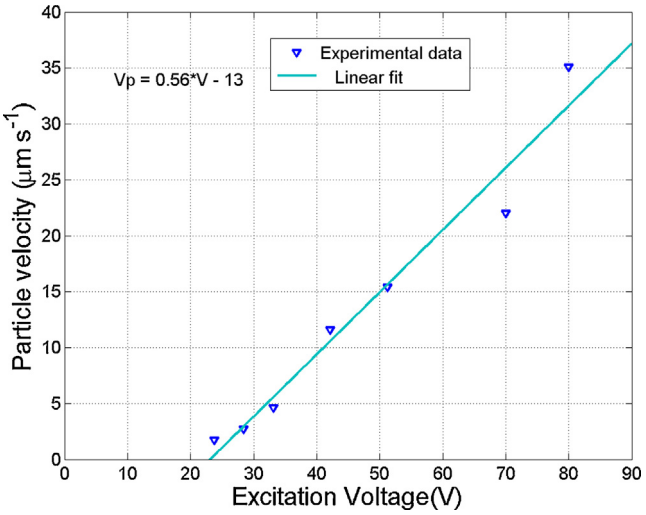

Fig. 11. Velocity as function of the excitation voltage.

are retraced and their velocity is estimated. Particle velocity as a function of the mixer excitation voltage is investigated.

As shown in Fig. 11, particle velocity increases with excitation voltage, which is an expected result since the vibration amplitude is proportional to excitation. However, it should be noted that we are characterizing the mixing behavior in the observable interval. In fact, beyond 80 V peak to peak, the mixing process is too fast to be measured using classic visualization method. A Particle Image Velocimetry PIV method should be used to extend this study.

To verify liquid viscosity influence on particle behavior under acoustic excitation, solutions with different concentration in glycerol were prepared. The following measurements, presented in Fig. 12, were made under an excitation voltage of 24 V peak to peak. As expected, particle viscosity decreases with viscosity under constant excitation. In fact, high viscosity microdroplet mixing requires more energy, i.e. higher voltage.

3.2.2. Dorplet insulation quality

Since the acoustic mixer is dedicated to biological and chemical domains, strict exigencies have to be respected, such as temperature variation control, and sample preservation from contamination. Our transducer was designed to avoid the latter risk by

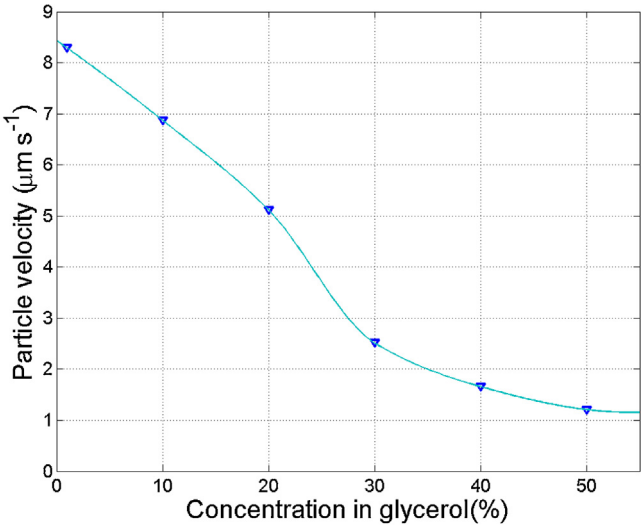

Fig. 12. Velocity as function of the droplet viscosity; Curve interpolation is made with a shape preserving one.

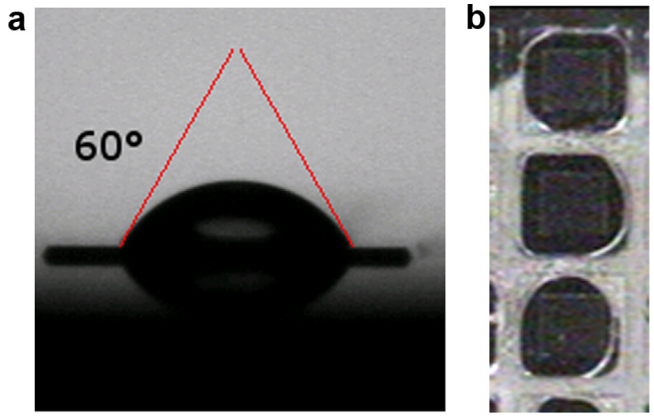

Fig. 13. (a) 400 nL water droplet contact angle measurement; (b) 400 nL droplets trapped between the transducer structure and a glass slide.

membrane structuration in wells. In planar operating, experimental surface characterization determined a 60° droplet contact angle using a fully automated drop tensiometer (Standard Tracker, Teclis ex. I.T. Concept, France). In this condition, 400–600 nL droplet is well received in etched well (Fig. 13a) without any noted contamination, regardless of the involved acoustic power.

Even in confined operating case, as the presence of a biochip in front of the acoustic mixer, drops are still well confined and take the well form. The experiment presented in Fig. 13b consists in the crushing of 400 nL water drops, previously positioned on the transducer active membrane by a glass slide moved accurately using a micropositioner. As shown, drops take the well form.

Nevertheless, with high acoustic energy, we notice liquid condensation on the glass slide. In planar operating case, the non-observation of liquid loss is not a proof of its absence. At this stage, doubt about the noted condensation nature is totally logic since the acoustic energy can induce both nebulization and evaporation phenomena. In both cases, it would be better to avoid great acoustic energies to avoid contamination during biological or chemical assays. Thermal measurements are performed to determine the exact nature of the observed phenomena.

3.3. Thermal effect of the acoustic mixing

3.3.1. Acoustic mixing as heating mechanism

Given the low volumes involved, conventional temperature measuring techniques would have disturbed the measurement by a probe insertion. This is why a distance measurement technique was preferred for the present study.

For that purpose, an infrared camera CEDIP, JADE, In–Sb focal plane array of detectors (3–5 μm spectral response, 240 × 320 pixels, pitch 30 μm) is placed in front of the acoustic mixer. IR cameras classically find application in process control, automation, solid temperature measurement, etc. But lately, it was applied in fluidic domain as a millifluidic calorimeter for the measurement of chemical reaction enthalpy and kinetics [19]. It was also used by Beyssen et al. to determine the heating effect of a SAW acoustic mixer [20].

In the linear approximation context, if the piezoceramic is subjected to a sinusoidal voltage, so is the membrane seat to sinusoidal vibration, whose amplitude is proportional to excitation. In the following experiment, 400 nL microdroplet temperature was measured while it is getting mixed under constant excitation voltage (35 V peak to peak for the experiment shown in Fig. 14).

Experiment showed that drop temperature increases under acoustic excitation which means that the observed liquid condensation in confined operating mode is due to evaporation. As shown

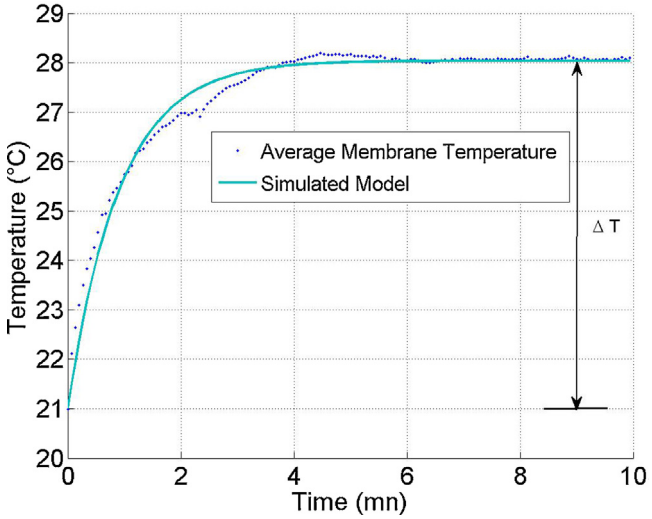

Fig. 14. 400 nL droplet temperature variation as function of time during acoustic mixing.

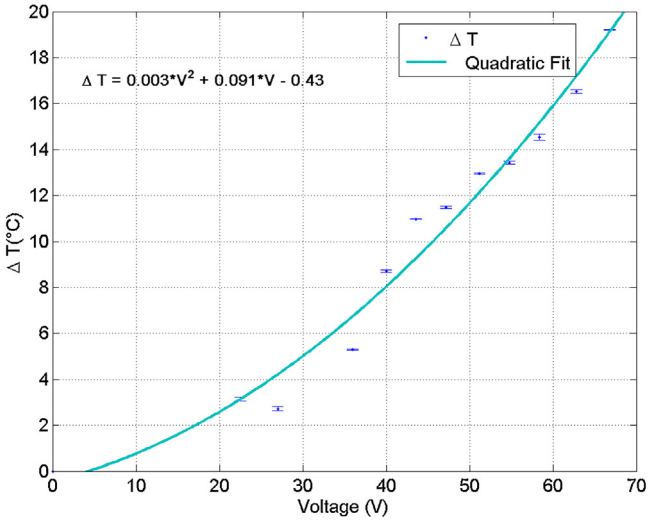

Fig. 16. Droplet maximum temperature variation ΔT as function of the transducer excitation voltage function.

in Fig. 14, the microdroplet temperature varies according to an exponential law as time function:

$$T\ (^{\circ}\mathrm{C}) = T_0 + K \times \left(1 - \exp\left(\frac{-t}{\tau}\right)\right); \quad (2)$$

where T_0 is the ambient temperature (°C), τ is a time constant (min^{-1}), and K is a constant.

Maximum variation in temperature ΔT is calculated according to the difference between the steady state and the ambient temperatures (initial drop temperature). Theoretically, drop temperature variation can have two possible explanations. First hypothesis consists in temperature rise of the vibrating membrane that induces heat conduction in the drop. The second possibility is that acoustic energy creates a thermal effect. To find out the correct explanation, we measured the vibrating membrane and the droplet temperatures in the same conditions. Fig. 15 shows temperature response of the vibrating membrane to cyclic excitation voltage. When excited, the acoustic mixer sees the membrane temperature increasing. Then, when the power is off temperature also decreases following an exponential law until resuming ambient temperature. While droplet temperature varies of about 7 °C, the vibrating membrane temperature variation does not exceed 1.25 °C which means that heating phenomenon is definitively due the created acoustic energy.

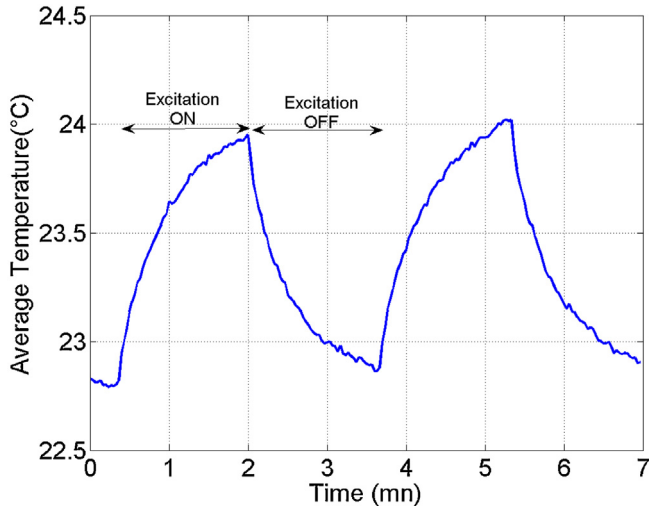

Fig. 15. Membrane temperature variation as function of time under cyclic excitation.

Fig. 16 demonstrates that drop maximum temperature variation ΔT increases with the excitation voltage and attends variations of about 20 °C compared to the ambient temperature. So, the acoustic transducer can be used as a droplet heating mechanism. A 2nd order polynomial law, as shown in Fig. 16, is sufficient to identify the experimental curve given that higher order coefficients are negligible (e.g. -6.7×10^{-5} as 3rd order coefficient) for the possible excitation voltage. For this experiment, to characterize drop temperature response to a given excitation voltage, a new drop is considered each time to avoid volume variation due to evaporation. The mixer is cleaned between successive experiments using a sulphuric acid solution in order to avoid surface condition changing.

3.3.2. *Mixing parameters for biological applications*

The aim behind using the acoustic transducer is to mix specific samples for biological or chemical operations. For that purpose, two operating modes are imaginable: The first one consists in taking back samples after homogenization using the acoustic mixer to perform the desired reaction, which will be a complicated process. The second possible operating mode would be to get sample mixed while biological or chemical reaction is performed, which is a real time operating mode.

Proceeding on mixing while biological operation is performed, means that a biochip is put in contact with drop top side while it is actively mixed. So, we consider for the following experiment a confined operating case. To achieve this, a framework is deposited around the well matrix to bring a glass slide which represents the biochip (Fig. 17). Thus, the distance separating the transducer from the glass slide is constant and equal to the thickness of the latter (160 μm).

In biological assays, temperature variation has to be negligible because it can, in certain cases, influence result by promoting a desired reaction or on the contrary by curbing it. In both cases, thermal effect would interfere with mixing influence and distorts our outcomes. Since our mixer produces a thermal effect depending on the excitation power, we have to find out an excitation regime where temperature variation in droplet is insignificant. We choose to excite the fundamental mode (18.74 kHz, 36 V peak to peak) since lower frequency modes require less excitation energy.

Because a microdroplet manual spotting is used for the preliminary biological assays, we choose to work on only 5 samples for the

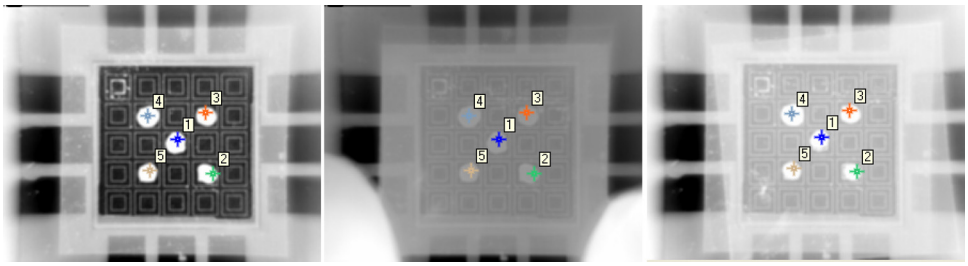

Fig. 17. Deposition of a glass framework, five microdroplets and then a glass film representing the biochip on the vibrating membrane.

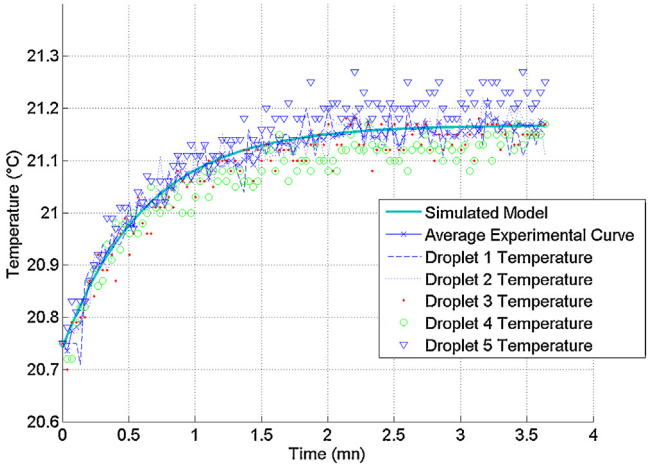

Fig. 18. Droplet temperature variation as function of time under acoustic excitation.

following experiment. Fig. 17 shows droplet disposition and their numeration.

Fig. 18 presents sample temperature variation. The five curves, corresponding to the five droplets temperature, are indistinguishable which means that droplet temperature behavior does not depend on its disposition on the vibrating membrane. Curves do follow the exponential law given in Eq. (2) (with the following characteristics for the main curve $T_0 = 20.74\,^{\circ}C$, $\tau = 0.6267\,min^{-1}$, and $K = 0.428$).

Two minutes after the experiment beginning, droplet temperature stabilizes. The maximum temperature variation in droplet is about 0.5 °C which is usually acceptable in biological and chemical operations.

Comparing our thermal characteristics to those presented by Beyssen for a SAW acoustic mixer [20], we notice that in both cases droplet temperature: varies following an exponential law, depends on excitation power, is independent from liquid volume, and can attend high values (30–80 °C depending on liquid viscosity and excitation power). In our case, droplet takes about 2 mn to reach its final temperature whereas it takes only few seconds under SAW excitation. Both mixers can be used as heating systems and can be carefully adapted to lab on chip applications.

4. Conclusion

At micro- and nano-scale, fluid mixing is a difficult challenge particularly in discrete microdroplets and especially in planar operating. In those conditions, absence of natural turbulence, evaporation, and contamination are challenges to overcome. Our low frequency acoustic mixer creates turbulence in 25 microdroplets simultaneously. The rapidity of drop homogenization and particle speed depend on the plugged acoustic energy which is in linear approximation proportional to excitation voltage. Experimentations showed that those velocities increase with excitation and decrease with liquid viscosity. However, thermal phenomenon appears and increases with the plugged energy. Measurements with IR camera proved that liquid temperature increases with excitation voltage. So, for biological and chemical operation sensitive to temperature, the acoustic mixer excitation parameters have to be carefully chosen in order to minimize the thermal effect which consequently means lower velocities set in. However, this study gives a velocity order of magnitude in the observable interval with a classic CCD camera. PIV measurement technique will be developed to characterize high velocity mixing. Future works will concern the comparison of experimental data with a model describing the observed hydrodynamic flows within the droplet matrix.

Acknowledgments

The authors would like to thank Vincent Placet for his assistance with IR camera and Valérie Petrini for her help in using the Flipchip system. We also thank the technologic platform MIMENTO (Besançon, France).

References

[1] A.E. Kamholz, B.H. Weigl, B.A. Finlayson, P. Yager, Quantitative analysis of molecular interaction in a microfluidic channel: the t-sensor, Anal. Chem. 71 (23) (1999).
[2] M.K. Tan, J.R. Friend, L.Y. Yeo, Surface acoustic wave driven microchannel flow, in: 16th Australian Fluid Mechanics Conference Crow Plaza, Gold Coast, Australia, 2–7 December, 2007.
[3] M.C. Jo, R. Guldiken, Dual surface acoustic wave-based active mixing in a microfluidic channel, Sens. Actuators A: Phys. 196 (2013) 1–7.
[4] A.R. Rezk, A. Qi, J.R. Friend, W.H. Lib, L.Y. Yeo, Uniform mixing in paper-based microfluidic systems using surface acoustic waves, Lab Chip 12 (2012) 773–779.
[5] M.K. Tan, L.Y. Yeo, J.R. Friend, Rapid fluid flow and mixing induced in microchannels using surface acoustic wavesRapid fluid flow and mixing induced in microchannels using surface acoustic waves, EPL 87 (2009) 47003–47008.
[6] A.-A. Deshmukh, D. Liepmann, A.-P. Pisano, Continuous micromixer with pulsatile micropumps, in: IEEE Workshop on Solid State Sensor and Actuators, Hilton Head Island, SC, 2000, pp. 73–76.
[7] T. Fujii, Y. Sando, K. Higashino, Y. Fujii, A plug and play microfluidic device, Lab Chip 3 (2003) 193–197.
[8] S.-C. Jacobson, T.-E. Mcknight, J.-M. Ramsey, Microfluidic devices for electrokinetically driven parallel and serial mixing, Anal. Chem. 71 (1999) 4455–4459.
[9] K. Yasuda, Non-destructive, non-contact handling method for biomaterials in micro-chamber by ultrasound, Sens. Actuators B: Chem. 64 (2000) 128–135.
[10] H.-H. Bau, J.-H. Zhong, M.-Q. Yi, A minute magneto hydrodynamic (MHD) mixer, Sens. Actuators B: Chem. 79 (2001) 207–215.
[11] H. Song, M.R. Bringer, J.D. Tice, C.J. Gerdts, R.F. Ismagilov, Experimental test of scaling of mixing by chaotic advection in droplets moving through microfluidic channels, Appl. Phys. Lett. 83 (22) (2003).
[12] P. Paik, V.K. Pamula, M.G. Pollack, R.B. Fair, Electrowetting-based droplet mixers for microfluidic systems, Lab Chip 3 (2003) 28–33.
[13] E.N. Wang, M.A. Bucaro, J.A. Taylor, P. Kolodner, J. Aizenberg, T. Krupenkin, Droplet mixing using electrically tunable superhydrophobic nanostructured surfaces, Microfluid. Nanofluid. 7 (2009) 137–140.
[14] A. Lee, A. Lemoff, R. Miles, Maghetohydrodynamic (MHD) driven droplet mixer, WO 03/078040 Al (2003).
[15] U. Lehmann, S. Hadjidj, V.K. Parashar, A. Rida, M. Gijs, Two dimensional magnetic manipulation of microdroplets on a chip, in: Proceedings of Transducers'05, Seoul, South Korea, 2005, pp. 77–80.
[16] A. Wixforth, Acoustically driven planar microfluidics, Superlattices Microstruct. 33 (2003) 389–396.

[17] F. Kardous, A. Rouleau, B. Simon, R. Yahiaoui, J.-F. Manceau, W. Boireau, Improving immunosensor performances using an acoustic mixer on droplet microarray, Biosens. Bioelectron. 26 (4) (2010) 1666–1671.
[18] F. Kardous, L. El Fissi, J.-M. Friedt, F. Bastien, W. Boireau, R. Yahiaoui, J. Manceau, S. Ballandras, Integrated active mixing and biosensing using low frequency vibrating mixer and Love-wave sensor for real time detection of antibody binding event, J. Appl. Phys. 109 (9) (2011) 094701–094708.
[19] C. Hany, C. Pradere, J. Toutain, J.C. Batsale, A millifluidic calorimeter with InfraRed thermography for the measurement of chemical reaction enthalpy and kinetics, QIRT 5 (2) (2008) 211–227.
[20] D. Beyssen, L. Le Brizoual, P. Alnot, I. Perry, Système de chauffage de goutte basé sur l'interaction SAW-liquide, Houille Blanche 6 (2007) 64–69.

Biographies

Faten Kardous was born in Tunis (Tunisia) in 1983. She received her Engineering Diploma from the ENSEEHIT Engineering School in Toulouse (France) in 2007. In the same year, she obtained her Master Degree of Science from the Polytechnic National Institute (INP) of Toulouse. She obtained her Ph.D. from the University of Franche-Comte in Besancon (France). Since 2011, she has been working as an Assistant Professor at The High Institute of Computer Science and Multimedia of Gabes (ISIMG), Tunisia. Her current research interests are investigating acoustic interaction with fluids, developing acoustic transducers and microfluidic devices for lab-on-chip applications devoted to biology.

Réda Yahiaoui received the M.S. degree in Electronics Sensors and Integrated Circuits – Option Microwaves and Fast Electronic in 1998. He obtained his PhD in Engineering Science in 2002, from the Paris-XI University in Orsay (France). He worked as Research Engineer in Electronics and project management in UAV development until 2005. Actually, he works as an Assistant Professor in the Micro Nano Sciences & Systems department (MN2S) of FEMTO-ST Institute in Besancon (France). His main interests are in fluidic MEMS design, fabrication and modelling.

Boujemaa Aoubiza was born in Taounate, Morocco, on January 1, 1964. He received his master degree in 1987 and his Ph.D. degree in 1991 in computational mathematics from the University of Besancon, France. Since 1994, he worked as a research and teaching assistant at the same university.

In the Besancon mathematics laboratory, his main research interests are in numerical simulation techniques applied in various field.

Jean-François Manceau was born in 1968; he received the Aggregation Degree in electrical engineering from the Ecole Normale Supérieure de Cachan in 1991 followed by the DEA (Master) degree in 1992. He moved to Besançon (France) to work on ultrasonic micro-actuators and obtained his Ph.D. from the University of Franche-Comté in 1996. At the present time, he is Professor at the University of Franche-Comté. His current researches concern acoustic interactions with fluids applied to sensors or actuators and design of micro-actuators for microfluidic applications within the Micro Nano Sciences & Systems (MN2S) Department of FEMTO-ST Institute.